Magnetically driven three-dimensional manipulation and inductive heating of magnetic-dispersion containing metal alloys

Citation: Calabro, Joshua D. et al. "Magnetically driven three-dimensional manipulation and inductive heating of magnetic-dispersion containing metal alloys." Proceedings of the National Academy of Sciences 107.11 (2010): 4834 -4839. Copyright ©2010 by the National Academy of Sciences

As Published: http://dx.doi.org/10.1073/pnas.1001410107

Publisher: National Academy of Sciences

Persistent URL: http://hdl.handle.net/1721.1/60944

Version: Final published version: final published article, as it appeared in a journal, conference proceedings, or other formally published context

Magnetically driven three-dimensional manipulation and inductive heating of magnetic-dispersion containing metal alloys

Joshua D. Calabro[a], **Xu Huang**[a], **Brian G. Lewis**[a], **and Ainissa G. Ramirez**[a,b,1]

[a]Department of Mechanical Engineering, Yale University, New Haven, CT 06520; and [b]Department of Materials Science and Engineering, Massachusetts Institute of Technology, Cambridge, MA 02139

Communicated by Walter L. Brown, Lehigh University, Berkeley Heights, NJ, February 4, 2010 (received for review March 20, 2009)

Fundamental to the development of three-dimensional microelectronic fabrication is a material that enables vertical geometries. Here we show low-melting-point metal alloys containing iron dispersions that can be remotely manipulated by magnetic fields to create vertical geometries and thus enable novel three-dimensional assemblies. These iron dispersions enhance the mechanical properties needed for strong, reliable interconnects without significantly altering the electrical properties of the alloys. Additionally, these iron dispersions act as susceptors for magnetic induction heating, allowing the rapid melting of these novel alloys at temperatures lower than those usually reported for conventional metal alloys. By localizing high temperatures and by reducing temperature excursions, the materials and methods described have potential in a variety of device fabrication applications.

3D structures | magnetic induction heating | magnetic manipulation | magnetorheological fluids

In practice, the creation of conductive three-dimensional pathways for today's microelectronic devices relies on the stacking of two-dimensional photolithographically placed layers or the creation of perpendicular vias (1). These multistep processes beg for a simpler and more cost-effective approach. Several new strategies have been proposed, including self-assembly (2), ink-jet printing (3), and multiphoton-absorption photopolymerization (4, 5). These techniques are certainly appealing for the fabrication of a new paradigm of devices (6). However, these techniques employ processes and materials not commonly found in today's microelectronics industry and may not allow one to deposit or move materials accurately. Here we report magnetically responsive, low-melting-point metal alloys (consisting of magnetic particles in a metal matrix) that can be manipulated remotely using a magnetic field. These materials will enable the movement of metal into vertical geometries and hard-to-reach locations (such as vias or channels) in electronic assemblies. These alloys also display enhanced mechanical strength for strong interconnects and allow direct heating by magnetic induction. This localized heating makes possible the assembly of the temperature-sensitive devices commonly found in optoelectronics.

Many low-melting-point alloys, such as bismuth- and indium-based alloys, can be altered by these methods. However, we used tin-silver based alloys as they have received recent attention by the electronics industry for their use as solders. Solders remain a ubiquitous joining material for the construction of modern electronics, serving as interconnects by providing conductive pathways (7). Traditionally, they are lead-based alloys. However, environmental and human health concerns have engendered a need for their replacement and recent restrictions in both Japan and the European Union necessitate a switch to lead-free solders (8). Unfortunately, the most suitable lead-free replacement, Sn-3.5%Ag, has a melting point of 220 °C, nearly 40 °C higher than the incumbent SnPb alloy (183 °C). In addition, Sn-3.5% Ag alloys requires even higher processing temperatures, which are often 30–40 °C above the melting point and can adversely affect device performance (9). These thermal excursions, along with the need to match the reliability and mechanical properties of SnPb, present a major challenge in the search for leaded-solder alternatives (9). The materials we present here provide a superior solution to this leaded-solder problem. We have found that the inclusion of magnetic particles in tin-silver-based alloys directly enhances mechanical strength while allowing localized heating using magnetic induction.

The inclusion of dispersions or particles into lead-free alloys has received recent attention, as a method to match the mechanical properties of lead-based materials. Dispersions act as obstacles and impede dislocation movement. (10) A variety of additives have been used to improve the mechanical properties of solder (11): oxide nanoparticles (Al_2O_3 and TiO_2) (12); intermetallic particles (Cu_6Sn_5) (13–15); metallic particles (Cu, Ag, Ni) (11, 16), NiTi shape-memory alloys (17), and carbon nanotubes (18). Other researchers have used nanodispersions of silver nanoparticles (11), Al_2O_3 nanoparticles (11), and nanostructured organic–inorganic hybrid polymers (like POSS) (19) in an effort to modify mechanical properties. Such additions have shown great promise in tailoring the mechanical performance of these alloys (11); however, little work has been done to address the thermal behavior of these materials.

To address this issue, it is proposed that iron dispersions will act as susceptors for magnetic induction heating, allowing the rapid melting of these novel alloys at lower temperatures than those usually reported for conventional solders. During inductive heating in an alternating magnetic field, metal alloys with magnetic dispersions are additionally heated by hysteresis losses (20). Such capabilities have potential in localizing high temperatures and reducing temperature excursions and are thus suitable for the assembly of temperature-sensitive devices. The use of solder is undergoing a paradigm shift in 3D fabrication: from self-assembly (2) to microsolidics (i.e., flexible conductive paths formed by vacuum-drawn solder in microfluidic channels) (21). Here we show another method to modify solder materials so that they respond to remote stimuli, particularly a magnetic field, enabling the ability to direct them with precision. These proof-of-principle experiments show that such solders—with their tailorable mechanical properties, their ability to move vertically and to create high-aspect ratio geometries, and their capacity for selective noncontact heating—are applicable to device fabrication.

Materials

Magnetically responsive, low-melting point metal alloys (solders) were prepared by incorporating multidomain magnetic dispersions into tin–silver

---

Author contributions: A.G.R. designed research; J.D.C., X.H., B.G.L., and A.G.R. performed research; J.D.C., X.H., B.G.L., and A.G.R. analyzed data; and J.D.C. and A.G.R. wrote the paper.

The authors declare no conflict of interest.

[1]To whom correspondence should be addressed. E-mail: ainissa.ramirez@yale.edu.

This article contains supporting information online at www.pnas.org/cgi/content/full/1001410107/DCSupplemental.

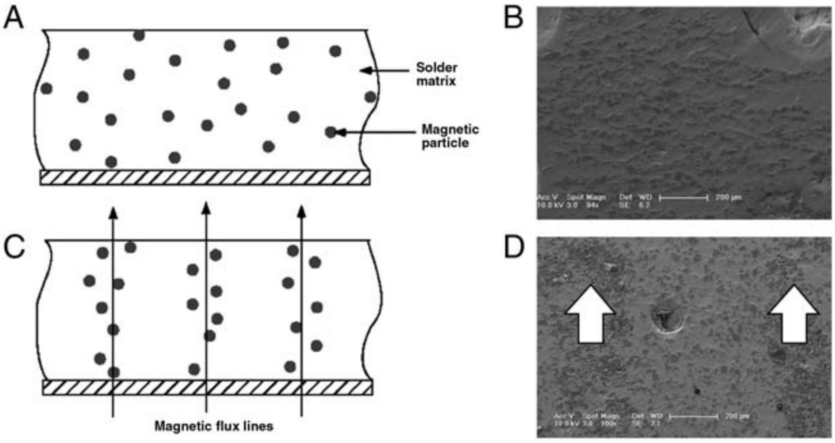

Fig. 1. Magnetic dispersions suspended in the molten metal matrix can assume several arrangements. (*A*) Dispersions can be randomly distributed. (*B*) SEM showing magnetic particles (*Dark Gray Spots*) homogenously incorporated in the SnAg matrix (*Light Gray Region*). (*C*) With suitable magnetic field, the magnetic particles cluster along the flux lines to form columns. (*D*) An SEM micrograph illustrating alignment throughout the thickness of the alloy (*White Arrows* indicate columns).

alloys (of the composition of Sn-3.5%Ag). Approximately 1–25% by weight of iron spheres at 325 mesh ($\phi \leq 44$ microns) were thoroughly mixed into Sn-3.5%Ag powder; after crushing and mixing, the iron particles were randomly oriented. To improve incorporation of the particles and the adhesion of the solder, ammonium chloride was added to the dry mixture as a cleaning agent (or flux) to remove the oxide on the iron particles. We prepared master batches of the mix, later diluting them to the desired dispersion concentration. Upon heating of the mixture, the iron particles do not dissolve into the matrix, as iron has limited solubility in both tin and silver (22). It is important to note that there is a negligible effect on the magnetic properties of iron at the melting point of Sn-3.5%Ag (220 °C), as iron has a Curie temperature of 770 °C (23).

A homogeneous distribution can be achieved by these methods, as shown schematically in Fig. 1*A*. This distribution can be seen in an SEM (Fig. 1*B*). Dark gray spots (iron particles) are embedded in a light gray matrix of tin–silver. It is possible to align the iron dispersions within the metallic alloy using a magnetic field (Fig. 1*C*) (16). Upon application of a suitable unidirectional magnetic field, the iron particles move into a stable configuration that minimizes the magnetostatic energy (23). Columns of spheres are magnetized in the same direction and the magnetic pole interactions between the chain of spheres cause them to repel each other until an equilibrium spacing is reached (16). Samples with these aligned configurations were generated by solidifying in a unidirectional magnetic field of 2,500 Gauss. An SEM micrograph (Fig. 1*D*) shows the resulting vertical columns of these aligned iron dispersions. The dark band of gray spots (iron particles) has a higher concentration along the field lines, indicated by the arrows.

Results and Discussion

Remote Vertical Manipulation. The incorporation of magnetic particles allows us to manipulate the molten alloy. Fig. 2 shows a reservoir of molten metal rising up in <1 s toward a ceramic magnet hovering 1 cm above it. We were also able to shift the solder stream, laterally (see Movie S1).

We constructed a variety of structures using these magnetically responsive materials. By means of a 2,500 G magnet, molten solder was drawn directly through holes (vias) 500 μm in diameter through a 400 μm-thick silicon wafer (Fig. 3*A* and *B*). These vias were made by deep reactive ion etching and were not coated with copper. Molten alloy was similarly drawn into the channels of a polydimethylsiloxane (PDMS) mold; the channels are as narrow as 700 μm in diameter and up to 4 mm deep. The resulting shapes were released once the molds reached room temperature. Fig. 3*C* shows the creation of a “Y” using this method; the extracted shape (Fig. 3*D*), indicates that lateral movement is possible. Interestingly, when the alloy is unconfined and a higher magnetic field (3,000 G) is applied, the dispersions surpass the surface tension of the molten alloy and move upward following the magnetic flux lines to create the “porcupine” shape that is often associated with ferrofluids (Fig. 3*E*). This phenomenon allows the generation of sharp tips and, unlike ferrofluids, this shape can be maintained by solidification at room temperature and is thus a method for creating novel electronic devices.

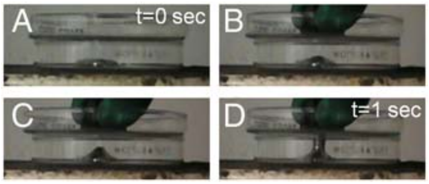

Fig. 2. (*A*) Vertical movement of a magnetically responsive low-melting-point alloy under the application of a common 1,000 G ceramic magnet. A sequence of images taken over a 1 s time period showing the solder rising up toward a magnet.

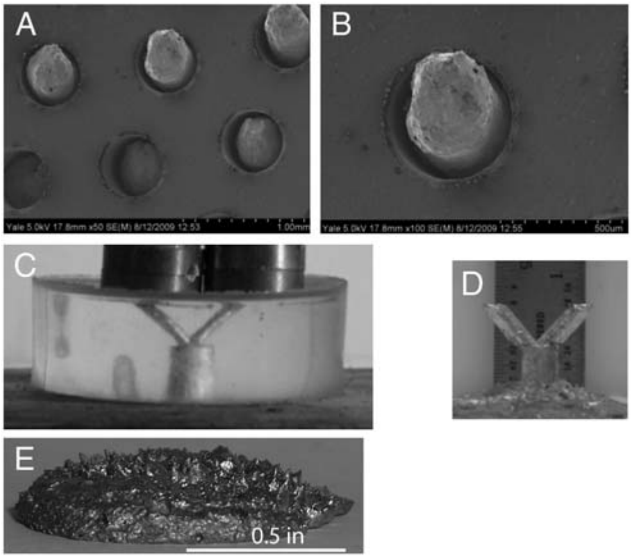

Fig. 3. An array of structures made with magnetically responsive solders. (*A*) SEM micrographs of silicon vias that have been filled with these materials. (*B*) The same vias at a higher magnification. (*C*) A three-dimensional structure rapidly generated with a magnetically responsive alloy in a PDMS mold. Molten alloy was drawn from a reservoir into a Y-shaped cavity within PDMS using samarium cobalt magnets. (*D*) The extracted Y-shape after solidification of the alloy. (*E*) Without containment these materials can achieve a “spiky” morphology often associated with ferrofluids, indicating the magnetic energy outweighs the sum of the surface and gravitational energies.

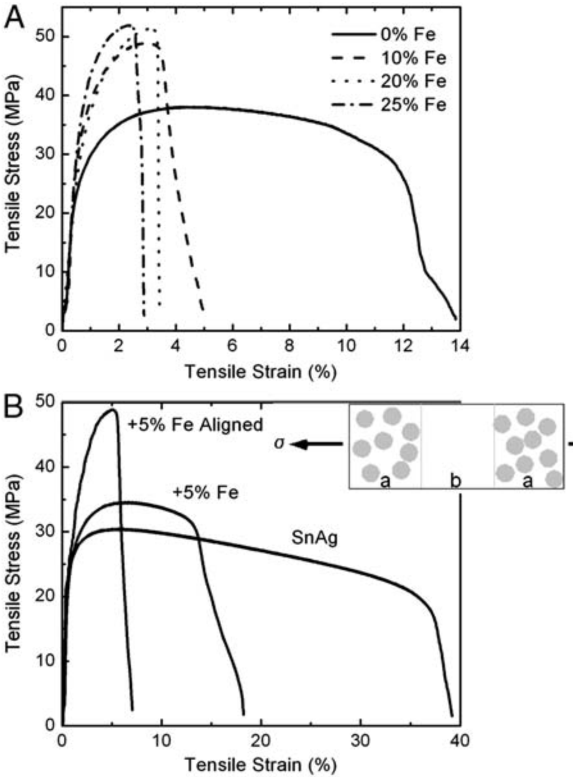

Fig. 4. Mechanical behavior at room temperature of dispersion-containing alloy tensile samples. (*A*) Stress-strain curves for SnAg alloy with increasing amounts of iron dispersions. (*B*) The role of aligned particles was also tested. Stress-strain curves for a SnAg + 5 wt.%Fe sample cast within a magnetic field (*Aligned Orientation*) and without a magnetic field (*Random Orientation*). A sample without dispersions is included for comparison. A schematic of a composite sample with (*a*) hard layers (*Particle-Rich Regions*) and (*b*) a soft layer (*Particle-Depleted Regions*) is in the inset.

Mechanical Properties. To determine the impact of dispersions on the mechanical properties, we used an Instron 5569 Universal Tester at a 0.0002/s strain rate. Samples of various dispersion concentrations were heated to 250 °C for 5 min and cast in a heated aluminum mold to produce American Standard of Testing and Measurement (ASTM) standard dog-bone specimens (32 mm × 6 mm) (24). Tensile tests were performed at 25 °C. We found that the incorporation of dispersions dramatically increases mechanical strength (Fig. 4*A*). The ultimate tensile strength, or UTS, (the curve height) is improved by nearly 40% over the dispersion-free samples; however, the ductility (the curve length) decreases as the dispersions provide more sites for void formation, coalescence, and fracture (10). The elastic modulus increases monotonically with increasing amounts of dispersions. Table 1 summarizes the average tensile properties of samples at different iron concentrations and shows that strength increases with dispersion concentration.

The mechanism by which the addition of particles changes the mechanical properties of these alloys is dispersion hardening. (10) Materials are strengthened by dispersions, which impede the motion of dislocations. During plastic deformation, dislocations move. When their movement is impeded, the material is strengthened and has increased yield and tensile strengths (10). To improve the mechanical and thermal stability of interconnects, the addition of dispersions to low-melting point alloys has been a recent research approach (11). As well as reducing dislocation motion, these dispersions act as nucleation sites, providing strength through the refinement of grains (25, 26). These fine-grained microstructures increase strength by a Hall–Petch mechanism, whereby grain boundaries impede dislocation motion (25, 26). Moreover, the dispersed iron particles also impede crack growth, grain coarsening, and the grain boundary sliding that can cause deformation under a constant load (or creep) (16).

The strength of a material can be further enhanced by the alignment of dispersions (Fig. 1*C* and *D*). Fig. 4*B* shows stress-strain curves of alloys with the same composition cast with and without a magnetic field and includes a dispersion-free sample for comparison. The alignment of dispersions has a marked effect. Note that the sample of only 5% iron by weight, when cast within a magnetic field, shows a 20% increase in strength. In these aligned-dispersion arrangements, the solder material acts as a composite consisting of hard layers (of particle-rich regions) and soft layers (of particle-depleted ones) (Fig. 4*B*). Plastic deformation in the soft layer is delayed by neighboring harder materials, by a mechanism called contact strengthening (27). In it, soft layers are constrained by the stronger nonyielding hard layers, which are still deforming elastically. The result is a triaxial tensile stress in the soft layer that minimizes the shear stresses in the soft layer that are required for plastic deformation (27). Contact strengthening allows tensile strengths many times higher than a whole sample made entirely of the soft layer material (27). This mechanism has been found to occur in laminates (28), joining materials (29), and in metal forming (10).

Electrical/Wetting/Hardness Properties. To be effective interconnect materials, the electrical resistivity and melting point of these new materials must not vary significantly from those of tin–silver. We found that the inclusion of magnetic dispersions does not alter these key properties of vertical connections. We evaluated the electrical properties by two-point probe measurements. After casting samples at various dispersion concentrations in a mold of known geometry, probes were attached to the ends of the sample and the voltage drop was recorded for varying currents[*]. The resistivity was then calculated for this known geometry and found to fall within the range of $5 - 10\ \mathrm{M}\Omega^{-1}/\mathrm{m}$, which is nominally the range for dispersion-free alloys (7). In an electrical circuit, these materials are neither deleterious to the circuit's performance, nor is there a detectable change in resistivity. We also determined the melting point using differential scanning calorimetry and found that the melting points of all the alloys studied remained at 220 °C. This result is expected because there is less SnAg material and the dispersions are not chemically active. Thus, the inclusion of dispersions, for the concentrations presented in this work, has little effect on these properties.

An alloy's ability to wet a surface is vital for creating electrical contacts. When we evaluated the wetting behavior by measuring the contact angle of approximately 0.05 g of molten alloy on a copper substrate, we found it unchanged for concentrations of up to 10 wt.% Fe (Table 1). At greater dispersion concentrations, the wetting angle increased monotonically. The hardness of these materials was also insensitive to the addition of dispersions of up to 10 wt.% Fe. Using a microindentor (measuring on the Vickers hardness scale) with a load of 100 g, it was found that the hardness of SnAg + 10%Fe (16.34 ± 0.66 HV) was nearly equivalent to SnAg (15.74 ± 0.47 HV). At 20 wt% Fe, i.e., double the concentration of dispersions, the hardness nearly doubles to 27.15 ± 0.76 HV (Table 1).

Induction Heating. Inductive heating of metals has largely been applied to heating of large scale workpieces, from fasteners to aerospace engine blades to automotive assemblies (30). It also has numerous biomedical applications for noncontact, localized heating and has been demonstrated to selectively heat cancerous cells (31) and to induce shape-memory effects in shape-memory

---

[*] In some cases, magnetic particles were aligned into columns within the sample by being cast in a magnetic field; measurements were taken perpendicular to the columns of aligned particles.

Table 1. Mechanical, electrical, and wetting properties of magnetically responsive alloys.

Sample (SnAg + wt.% Fe)	Modulus (MPa)	UTS (MPa)	Elongation (%)	Conductivity($M\Omega^{-1}$/m)	Hardness (HV)	Contact angle (°)
0% Fe (SnAg)	5158	34.5 ± 2.2	25.7 ± 7.4	9.44 ± 02	15.74 ± 47	12.1 ± 1.7
5%	4992	36.8 ± 1.6	15.0 ± 1.6	–	16.86 ± 54	11.3 ± 0.9
5% aligned	–	48.7 ± 1.2	7.7 ± 2.1	–	–	–
10%	7977	44.8 ± 3.4	5.5 ± 1.0	8.32 ± 10	16.34 ± 66	11.7 ± 1.7
10% aligned	–	–	–	7.23 ± 16	–	–
20%	9564	50.9 ± 0.6	4.7 ± 1.4	6.43 ± 18	27.15 ± 76	23.4 ± 1.5
SnPb (literature)	–	–	–	5.58 (7)	13.1 (7)	16 (7)

polymers containing magnetic-nanoparticles (32). During induction, coils are driven by an ac power supply that generates a magnetic field and a workpiece placed inside of the magnetic field heats up from the hysteresis and eddy current losses (Fig. 5*A*). The heat loss, P, can be determined by

$$P = W_H f + k f^2 \qquad [1]$$

where W_H is the work done along the hysteresis loop, f is the frequency, and k is a constant that depends on the conductivity and the magnetic field (20). Induction heating can reduce the temperatures used in microelectronic fabrication and the sealing of its packages, thereby reducing warpage due to differences in thermal expansion.

In this work, we demonstrate proof of principle by showing that the particles within the metal matrix cause the metal to heat at a faster rate than materials without dispersions. As mentioned above, temperatures nearly 40 °C higher than those for the incumbent SnPb alloy (183 °C) are required to melt SnAg (MP = 220 °C) and its alloys. The incorporation of magnetic materials into these alloys that enables localized heating by magnetic induction mitigates this requirement. Fig. 5*A* is a schematic of our induction heating experiments, where both dispersion-free and magnetic dispersion-containing samples sit side by side under the same heating conditions. The surface temperature of 6 g samples, after being subject to the lowest setting of 12,150 Hz, 8 kW, 350 V of a foundry-grade Inductotherm VIP system 75-30-R for 1 min, was measured with an infrared camera. Iron-dispersion-containing alloys heat to a higher surface temperature (of 118 °C) in this test condition, nominally 70 °C higher than metals without dispersions. It is important to note that these are surface measurements. The dispersion-containing solder was hotter internally, as it was easily deformed when pressure was applied.

We also examined the effect of other magnetic dispersions, to explore the impact of hysteresis heating (the first term in Eq. **1**) and found that nickel dispersions can also produce significant heating; cobalt is the least effective heating dispersion under these test conditions (Fig. 5*B*). As expected, higher concentrations of magnetic Fe particles produced faster heating (Fig. 5*C*). Such improved heating performance could enable bonding at lower temperatures, thus limiting thermal damage. However, the ideal composition for use in microelectronics will need to trade-off heating efficiency with viscosity, which increases with dispersion concentration. (Additional work along these lines would include the exploration of low-frequency induction heating that would directly couple with the magnetic particles.)

Possible Applications. Materials that can be magnetically manipulated can enable innovation. We used them to create several devices, including a magnetic-sensor circuit that creates an open circuit when magnetic fields are encountered (Movie S2). We also demonstrated liquid conveyance of less-dense objects (a copper coin) in magnetically responsive molten metal (Movie S3). The application of a magnetic field aligns the dispersions, causing them to transport an object laterally. It is envisioned that such materials could be used for self-healing assemblies; defective joints that cause open circuits could be "healed" by minimized heating in a magnetic field (16), obviating the arduous process of removing and resoldering components. Experiments at this level of fabrication still need to be performed.

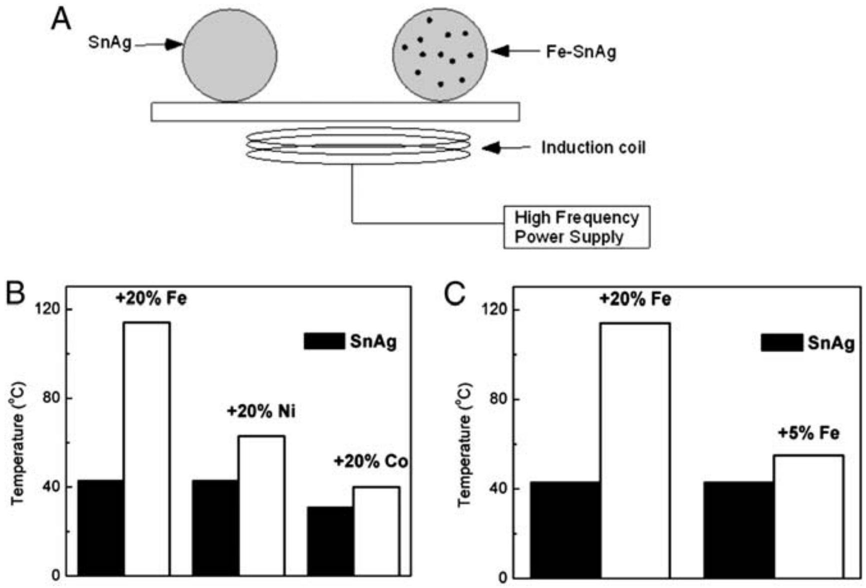

Fig. 5. An experimental setup to test the magnetic induction heating response of solder with and without magnetic dispersions. (*A*) An illustration of a magnetic induction heating experiment showing two samples (one with and one without dispersions) under the same induction conditions. Magnetic induction heating responses of studied alloys with (*B*) dispersions of different magnetic elements and (*C*) iron dispersions at different concentrations.

This further experimentation is in line with the requirements for the general conversion to lead-free solders (33). New materials, such as the one that we have formulated, lead to new developments in manufacturing (including interconnection) in that they differ from traditional solder materials in a variety of ways. Solidification behavior, mechanical and creep properties, fracture toughness, coefficient of thermal expansion, and microstructural stability, each of which affect the resulting stress levels in the solder and in turn its performance (34), may each be different. The synthesis and properties exhibited here provide the key first steps to this potential paradigm shift in microelectronics fabrication. We do not underestimate the challenges to industrial-scale production that changes in material properties imply, but we are confident that following further investigation, these materials will be successfully adopted for use.

Conclusions

In view of the need for the robust assembly of three-dimensional interconnects, the materials and methods described in this paper show that magnetically responsive, low-melting point alloys (or solders) have the ability, in an accessible way, to create 3D geometries. In addition, our novel SnAg-based alloys, with the addition of iron particles, can be heated without damaging adjacent components and have superior mechanical properties. These methods suggest new routes for creating conductive paths and performing microelectronic repairs. With the capabilities demonstrated here, a range of devices with new functionalities is possible. These lead-free alloys are useful both for current challenges in interconnects and have novel utilities for additional applications.

Experimental Methods

Tensile Testing. Tensile specimens were produced by first grinding Sn-3.5% Ag solder powder (Kester), 325 mesh iron powder (Alfa Aesar), and granular ammonium chloride with a mortar and pestle. The powder mixture was poured into preheated graphite crucibles and heated until a composite solder bead formed, which was then quenched in water. The beads thus formed were used as master batches and were mixed with the appropriate amount of SnAg ingot solder to yield the desired dispersion concentrations. Blank SnAg samples were produced using the same process, a combination of solder powder beads and ingot solder. The solder was cast into a heated aluminum mold (approximately 250 °C) lined with graphite powder, which was used as a releasing agent. The dimensions of the mold conformed to a dog-bone sample shape given by ASTM E8M-04. (24) While cooling, the solder was agitated slightly by tapping the mold to reduce void formation. After the solder solidified, the mold was quenched and the specimen removed with a hammer and punch. Testing was performed with the Instron 5569 Universal Tester at a 0.0002/s strain rate.

Fabrication of Aligned Samples. Magnets were used during solder solidification to investigate dispersion alignment. Two magnets, one above the gauge section and one below, were placed on the mold as the tensile specimen cooled. A glass petri dish was placed on top of the mold to protect the specimen's shape, and the two magnets were clamped onto the gauge section. The magnets were samarium cobalt discs (.375" diameter and .250" thickness), with a maximum energy product of 18 MGOe.

Contact Angle Measurements. Copper substrates were first cleaned with acetone in an ultrasonic cleaner, placed onto a 300 °C hotplate, and coated liberally with Johnson's Original Soldering Fluid (zinc chloride and ammonium chloride). A small piece of solder (<0.05 g) was removed from specimens after tensile testing and placed onto the copper. The solder melted undisturbed and remained on the hotplate for an additional 30 s. Contact angles were measured using AST Products' VCA2500 Video Contact Angle System.

Hardness Testing. Small pieces of solder were clipped off of the ends of tensile specimens post tensile testing. The samples were placed into Allied 1¼" Diameter Mount Protection Caps, which were then filled with Allied EpoxySet (Resin, #145-20015 and Hardener, #145-20020). The mounts were heated to approximately 100 °C to accelerate solidification. Once solid, the mounts were cut away and the epoxy and solder were polished. Testing was performed using a Wilson–Wolpert Microindentation Tester 402MVD with a 10 s dwell and 100 gf load. Each of the solder compositions was tested ten times, with the mean hardness values given in Table 1.

Fabrication of Microfluidic Channels. We fabricated polymeric molds of polydimethylsiloxane (PDMS) with templates in the desired "Y" shape. Three metal wires were put into place and freshly mixed PDMS (Sylgard 184, Dow Corning, Inc.) was poured and thermally cured (80 °C, 8 hr). Once the PDMS solidified, the wires were then individually pulled out to form a Y-shaped cavity.

Casting of Solder. We placed the polymeric mold over a reservoir of molten magnetic solder on a hot plate. We applied a magnetic field on top of the mold, using a 2,500 G magnet. In experiments the solder filled the cavity completely. In some cases, the magnets needed to be moved to provide a sufficient field for the solder to traverse sharp (corner) geometries. The solder was found to wet the entire cavity.

Induction Heating Measurements. Dispersion-containing and dispersion-free samples were polished to a pristine surface to remove surface oxide. Both samples were placed on a fire brick and subjected to the lowest setting of a foundry-grade Inductotherm VIP system 75-30-R at conditions of 12,150 Hz, 8 kW, 350 V for 1 min in Fig. 5*A*. The induction heater was turned off and the surface temperature was measured with an infrared camera (Informatrics Inc.) as a function of time and the video was recorded and time-stamped. A line profile was generated and the peak temperatures were plotted for each test (Fig. 5*B* and *C*).

ACKNOWLEDGEMENTS. We thank M. Tarkanian for the generous use of his equipment. We are indebted to S.M. Allen and E.L. Hayes for fruitful discussions. This work was made possible by Massachusetts Institute of Technology's Martin Luther King, Jr. Visiting Professorship Program, Yale University's Yale Institute for Nanoscience and Quantum Engineering Seed Award, and National Science Foundation Grant CMMI-0925994.

1. Jaeger RC (2001) *Introduction to Microelectronic Fabrication* (Prentice Hall, New York), 2nd Edition.
2. Gracias DH, Tien J, Breen TL, Hsu C, Whitesides GM (2000) Forming electrical networks in three dimensions by self-assembly. *Science* 289(5482):1170–1172.
3. Garnier F, Hajlaoui R, Yassar A, Srivastava P (1994) All-polymer field-effect transistor realized by printing techniques. *Science* 265(5179):1684–1686.
4. Maruo S, Nakamura O, Kawata S (1997) Three-dimensional microfabrication with two-photon-absorbed photopolymerization. *Opt Lett* 22(2):132–134.
5. Witzgall G, Vrijen R, Yablonovitch E, Doan V, Schwartz BJ (1998) Single-shot two-photon exposure of commercial photoresist for the production of three-dimensional structures. *Opt Lett* 23(22):1745–1747.
6. Yellen BB, Hovorka O, Friedman G, Swinney HL (2005) Arranging matter by magnetic nanoparticle assemblers. *Proc Natl Acad Sci USA* 102(25):8860–8864.
7. Evans JW (2007) *A Guide to Lead-free Solders* (Springer–Verlag, London) p 114.
8. Official Journal of the European Union (2003) *Directive on the Restriction of the Use of Certain Hazardous Substances in Electrical and Electronic Equipment* (European Union, Luxembourg).
9. Li YI, Moon KS, Wong CP (2005) Materials science: Electronics without lead. *Science* 308(5727):1419–1420.
10. Dieter GE (1986) *Mechanical Metallurgy* (McGraw–Hill, New York), 3rd Ed p 218.
11. Guo F (2007) Composite lead-free electronic solders. *J Mater Sci: Mater Electron* 18(1-3):129–145.

12. Mavoori H, Jin S (1998) New, creep-resistant, low melting point solders with ultrafine oxide dispersions. *J Electron Mater* 27(11):1216–1222.
13. Hwang S-Y, Lee J-W, Lee Z-H (2002) Microstructure of a lead-free composite solder produced by an in situ process. *J Electron Mater* 31(11):1304–1308.
14. Lee J-H, et al. (2000) Reflow characteristics of Sn-Ag matrix in situ composite solders. *Scripta Mater* 42(8):827–831.
15. Subramanian K, Bieler T, Lucas J (1999) Microstructural engineering of solders. *J Electron Mater* 28(11):1176–1183.
16. McCormack M, Jin S, Kammlott GW (1994) Enhanced solder alloy performance by magnetic dispersions. *IEEE T Compon Pack A* 17(3):452–457.
17. Dutta I, et al. (2004) Development of a novel adaptive lead-free solder containing reinforcements displaying the shape-memory effect. *J Electron Mater* 33(4):258–270.
18. Nai S, Wei J, Gupta M (2006) Lead-free solder reinforced with multiwalled carbon nanotubes. *J Electron Mater* 35(7):1518–1522.
19. Lee A, Subramanian K (2005) Development of nano-composite lead-free electronic solders. *J Electron Mater* 34(11):1399–1407.
20. Cullity BD (1972) *Introduction to Magnetic Materials* (Addison–Wesley, Reading).
21. Siegel AC, Bruzewicz DA, Weibel DB, Whitesides GM (2007) Microsolidics: Fabrication of three-dimensional metallic microstructures in poly(dimethylsiloxane). *Adv Mater* 19(5):727–733.
22. Massalski TB (1990) *Binary Phase Diagrams* (ASM International, Materials Park, OH), 2nd Ed.
23. Omar MA (1975) *Elementary Solid State Physics* (Addison–Wesley, Reading).
24. ASTM (2004) Standard Test Methods for Tension Testing of Metallic Materials [Metric]. *E8M-04* (American Society for Testing Materials International, West Conshohocken).
25. Hall EO (1951) The deformation and ageing of mild steel: III discussion of results. *Proc Phys Soc Lond B* 64:747–753.
26. Petch NJ (1953) The cleavage strength of polycrystals. *J Iron Steel I* 174(1):25–28.
27. O'Brien M, Rice CR, Olson DL (1976) High-strength diffusion welding of silver coated base metals. *Weld J* 55(1):25–27.
28. Trykov YP, Pavlov AI, Adamenko NA, Naumov AN, Sedov EV (1998) The strength increasing the laminated metal-polymer compounds. *Physics and Chemistry of Processing of Materials* 4:53–56 (in Russian).
29. Backofen WA (1972) *Deformation Processing* (Addison–Wesley, Reading).
30. Stansel N (1949) *Induction Heating* (McGraw–Hill, New York).
31. Bonder MJ, et al. (2006) In vitro heating with polyethylene glycol coated Fe nanoparticles. *IEEE T Magn* 42(10):3602–3604.
32. Mohr R, et al. (2006) Initiation of shape-memory effect by inductive heating of magnetic nanoparticles in thermoplastic polymers. *Proc Natl Acad Sci USA* 103(10): 3540–3545.
33. Stalter KA, Baggio T, Suetsugu K (2004) Pb-Free Component Conversion and Some Manufacturing Experiences. *Handbook of Lead-Free Solder Technology for Microelectronic Assemblies*, eds KJ Puttlitz and KA Stalter (Dekker, New York).
34. Handwerker CA, Suganuma K, de Kluizenar E, Gayle FR (2004) Major International Lead (Pb)-Free Solder Studies. *Handbook of Lead-Free Solder Technology for Microelectronic Assemblies*, eds KJ Puttlitz and KA Stalter (Dekker, New York) p 1026.